CYS3, a Hotspot of Meiotic Recombination in *Saccharomyces cerevisiae*: Effects of Heterozygosity and Mismatch Repair Functions on Gene Conversion and Recombination Intermediates

Michèle Vedel and Alain Nicolas

Institut Curie, Section de Recherche, Compartimentation et Dynamique Cellulaires, UMR144, Centre National de la Recherche Scientifique, 75248 Paris Cedex 05, France

Manuscript received September 10, 1997
Accepted for publication September 23, 1998

ABSTRACT

We have examined meiotic recombination at the *CYS3* locus. Genetic analysis indicates that *CYS3* is a hotspot of meiotic gene conversion, with a putative 5′–3′ polarity gradient of conversion frequencies. This gradient is relieved in the presence of *msh2* and *pms1* mutations, indicating an involvement of mismatch repair functions in meiotic recombination. To investigate the role of mismatch repair proteins in meiotic recombination, we performed a physical analysis of meiotic DNA in wild-type and *msh2 pms1* strains in the presence or absence of allelic differences at *CYS3*. Neither the mutations in *CYS3* nor the absence of mismatch repair functions affects the frequency and distribution of nearby recombination-initiating DNA double-strand breaks (DSBs). Processing of DSBs is also similar in *msh2 pms1* and wild-type strains. We conclude that mismatch repair functions do not control the distribution of meiotic gene conversion events at the initiating steps. In the *MSH2 PMS1* background, strains heteroallelic for frameshift mutations in *CYS3* exhibit a frequency of gene conversion greater than that observed for either marker alone. Physical analysis revealed no modification in the formation of DSBs, suggesting that this marker effect results from subsequent processing events that are not yet understood.

GENE conversion events, which represent the nonreciprocal transfer of information from one chromatid to another, are manifested during meiosis by the non-Mendelian segregation (NMS) of heterozygous markers. These NMS events are the signature of recombination in that they include the large majority of intragenic recombination events and are associated with the reciprocal exchange of flanking markers about half of the time (Fogel *et al.* 1981; Petes *et al.* 1991). In *Saccharomyces cerevisiae*, the average frequency of meiotic gene conversion at an individual site is 2–3% per meiosis, but it can vary from <1% to >50% (Fogel *et al.* 1981). At specific loci, gradients of conversion frequencies that vary in steepness from one locus to another have been detected: 1–10% across the *ARG4* locus (Fogel *et al.* 1981), 4–15% at *DED81* (Schultes and Szostak 1990), 5–14% at *HIS2* (Malone *et al.* 1992), 1–3% at *HIS1*, and 17–50% at *HIS4* (Petes *et al.* 1991). The molecular mechanism(s) that controls the steepness of these gradients is not yet understood. Two mechanisms have been proposed to explain shallow and steep gradients, respectively. Detloff *et al.* (1992) postulated that conversion of markers exhibiting low postmeiotic segregation (PMS) could reflect a preponderance of restoration-type over conversion-type repair. That is, mismatches located near the site of initiation might be repaired mainly by conversion-type repair. In contrast, if half of the distal mismatches were repaired by restoration-type repair, these events would not be detected and, consequently, would contribute to a twofold gradient, as observed at *HIS4*. Evidence for restoration-type repair at this locus has been shown recently (Kirkpatrick *et al.* 1998). Preferential repair resulting in restoration at the low end of the polarity gradient has been observed. Steeper gradients must result from another mechanism. They could be explained if recombination is initiated at fixed sites and if heteroduplex regions extend to varying distances from these sites. Deletion analyses have identified *cis*-acting regions required for high levels of gene conversion in small chromosomal regions located 5′ of the coding sequence of the *ARG4* (Nicolas *et al.* 1989; de Massy and Nicolas 1993) and *HIS4* (Detloff *et al.* 1992) genes. These positions are consistent with the observed gradient of gene conversion frequencies at these loci in that the highest frequency of conversion is at the 5′ end. In contrast, the conversion gradient associated with the *HIS2* hotspot is of opposite polarity, suggesting that some *cis*-acting sequences required for the high level of gene conversion at *HIS2* are located downstream (Malone *et al.* 1992, 1994; Bullard *et al.* 1996).

Genetic recombination in yeast is also characterized

Corresponding author: Alain Nicolas, UMR144, Institut Curie, Section de Recherche, 26 rue d'Ulm, 75248, Paris Cedex 05, France.
E-mail: anicolas@curie.fr

by the formation of DNA double-strand breaks (DSBs), which occur at recombination hotspots (Sun *et al.* 1989; Cao *et al.* 1990; Fan *et al.* 1995; Mao-Draayer *et al.* 1996) and at many locations in the genome, and it is likely that most if not all meiotic-recombination events are initiated by meiosis-specific DSBs (Zenvirth *et al.* 1992; Wu and Lichten 1994; Klein *et al.* 1996; Baudat and Nicolas 1997). The processing of DSBs yields single-strand tails (Sun *et al.* 1989; Cao *et al.* 1990) that invade the homologous chromosome, leading to the formation of Holliday junctions (Schwacha and Kleckner 1995) and heteroduplex DNA (Lichten *et al.* 1990). In the context of the DSB repair model (Szostak *et al.* 1983), gene conversion gradients could be explained by the distance between the site at which the heteroduplex DNA is initiated and a specific genetic marker undergoing conversion.

Conversion gradients are nearly abolished at both the *ARG4* and *HIS4* loci in mutants defective in the *MSH2* and *PMS1* mismatch repair (MMR) genes, which suggests a role for the MMR system in the formation of the conversion gradient (Alani *et al.* 1994). Msh2p, one of six homologs of the *Escherichia coli* MutS protein (Msh1p–Msh6p), is a central component of the *S. cerevisiae* MMR system (Reenan and Kolodner 1992a,b). It binds mispaired bases and recognizes both single base mispairs and multiple base insertion/deletion mispairs (Alani 1996). Mlh1p and Pms1p are homologs of the bacterial MutL protein (Kramer *et al.* 1989; Reenan and Kolodner 1992a). Genetic and biochemical analyses of MMR in *S. cerevisiae* have suggested that MMR involves two complexes: two MutS homologs (Msh2p and Msh3p or Msh6p) form a complex that recognizes mispairs, which in turn is bound by a complex of two MutL homologs (Mlh1p and Pms1p, Prolla *et al.* 1994; Marsischky *et al.* 1996). In addition, purified Msh2 protein binds to synthetic Holliday junctions (Alani *et al.* 1997). The Msh2p-Holliday junction complex appears to be more stable than the Msh2p-duplex DNA complex, suggesting that Msh2p could coordinate MMR and genetic recombination. The function of these MMR proteins with respect to gene conversion gradients, however, remains to be elucidated. Observations published by Alani *et al.* (1994) suggest that the existence of polarity reflects the frequency of heteroduplex formation and/or the processing of this recombination intermediate by MMR-dependent processes.

With the goal of defining the recombination intermediate(s) on which the MMR system acts, we have undertaken a genetical and physical characterization of gene conversion at the *CYS3* locus, which is proposed to be a hotspot of gene conversion (Cherest and Surdin-Kerjan 1992). Our results demonstrate that the *CYS3* locus is indeed a gene conversion hotspot, and that the Msh2 and Pms1 proteins act to control the frequency of gene conversion after the formation of initiating DSBs.

MATERIALS AND METHODS

Media and sporulation conditions: Standard medium (YPD) was used for vegetative growth. Presporulation medium was SPS, and sporulation was carried out in 1% potassium acetate, as described previously (de Massy and Nicolas 1993). The addition of 0.5 mm reduced glutathione to all media compensated for cysteine auxotrophy. The segregation of *cys3* mutations was determined using synthetic minimal medium without glutathione and supplemented for all other auxotrophic markers.

Plasmids: Fragments of the *CYS3* region were isolated from plasmid pStr1.1 (gift of Y. Surdin-Kerjan) and recloned in pMLC28 (Schultes and Szostak 1990) or pKS Bluescript. The *Eco*RI site of pMLC28 was first destroyed to simplify the construction of the *cys3-RI* strain. The *Pst*I and the two *Pst*I/*Hin*dIII fragments (see Figure 1) were inserted into pMLC28 to obtain pMV1, pMV2, and pMV3, respectively. The *CYS3* locus was reconstituted from pMV1 and pMV2 (2238 bp *Pst*I-*Xca*I fragment) to give pMV7.

The *cys3-Bg* and the *cys3-RI* strains were made using plasmids bearing a part of the mutated *CYS3* gene and the *URA3* gene. The *Bgl*II and the *Eco*RI mutations were made by filling in the relevant restriction site overhangs with Klenow DNA polymerase in pMV1 or in pMV7, respectively. An *Xba*I-*Sac*I fragment containing the *URA3* gene (from pHS113, Sun *et al.* 1989) was ligated into the *Xba*I-*Sac*I-digested *cys3-Bg* plasmid. The *Hin*dIII/*Xho*I fragment bearing the *Eco*RI mutation was isolated from pMV7 and ligated to the *URA3* plasmid described previously to generate the *cys3-RI* plasmid. All restriction enzymes were from New England Biolabs (Beverly, MA), with the exception of *Bst*1107I (Fermentas), which was used instead of *Xca*I. T4 DNA ligase and Klenow DNA polymerase were from Boehringer Mannheim (Mannheim, Germany).

Strains: *E. coli* strains were either DH5α or NPS RKII and were cultured in standard media (LB and 1% thymidine LB, respectively). All *S. cerevisiae* strains used were derived from the congenic MGD131-102A and MGD131-2C haploids (see Table 1). Genetic markers were introduced into the *CYS3* gene by a two-step replacement procedure using *URA3* as a selectable marker (Scherer and Davis 1979). Both *cys3-Bg* and *cys3-RI* plasmids were linearized by *Xho*I, and each of them was used to transform MGD131-102A and MGD131-2C haploids to uracil prototrophy. Ura^- derivatives were obtained from the primary transformants by selection with 5-fluoroorotate (Boeke *et al.* 1984). Both constructions were subsequently verified by Southern blot analysis of genomic DNA digested with *Cla*I (for the *cys3-Bg* mutation) or *Ase*I (for the *cys3-RI* mutation).

Strains heteroallelic for *CYS3* mutations in the *rad50S* background were obtained by crossing appropriate segregants from a cross between the *rad50S* strains ORT305 or ORT311 and a *cys3-Bg* or *cys3-RI* strain. A *msh2 pms1* homozygous diploid (ORD2048) was constructed by mating RKY1929 and RKY1939 (Alani *et al.* 1994). The homozygous *msh2 pms1 rad 50S* diploid ORD2047 was built with segregants from ORD2043 (RKY1935 × ORD311). The *msh2 pms1 rad50S* haploids ORD-2043-9B and ORD2043-13B were used to construct ORD2047, which is homozygous for all three mutations. The correct genotype of these strains was verified by PCR and Southern blot analysis using a radiolabeled 600-bp fragment generated with two oligonucleotides specific to the *MSH2* coding region.

Genetic techniques: Standard procedures for mating and tetrad dissection were used. Cells were grown in presporulation medium (SPS) and sporulated in 1% potassium acetate at 30°. Tetrads were generally dissected after 2–3 days in sporulation medium. Because *msh2* and *pms1* mutants display a mutator phenotype, *msh2 pms1* strains were mated and sporu-

lated after limited growth, as described previously (Reenan and Kolodner 1992b; Alani *et al.* 1994).

For tetrad analysis of diploid strains with two *cys3* mutant markers, tester strains ORD2017-1A (*his1 cys3-Bg MAT***a**), ORD-2022-1A (*his1 cys3-Bg MAT*α), ORD2031-1A (*his1 cys3-RI MAT***a**), and ORD2027-29A (*his1 cys3-RI MAT*α) were constructed. *cys3-Bg* or *cys3-RI* segregants were mated with the above strains. UV-induced Cys^+ papillations of resultant diploids allowed for the identification of haploid segregants carrying the *cys3-Bg* and *cys3-RI* mutation either singly or together. Meiotic viability of a diploid strain is defined as the percentage of tetrads with four viable spores among the total number of dissected tetrads.

Isolation of DNA and detection of DSBs: Twenty-five milliliters of meiotic cells were harvested from sporulation medium at each time point (0 to 24 hr). Spheroplasts were produced by incubation with Zymolyase (Chemical Credential, ICN) for 30 min at 30°. DNA was purified as described previously (de Massy and Nicolas 1993) using SDS, proteinase K, gentle phenol extractions, and ethanol precipitations. One to two micrograms of DNA were digested by an appropriate restriction enzyme, subjected to electrophoresis on a 0.8% agarose gel, and blotted onto a nylon membrane (Hybond-N+; Amersham, Rainaham, UK). The *CYS3* region was examined using the probes shown in Figure 1: (1) the downstream probe a, which is specific to the 3′ end of *CYS3* and part of the *FUN36* ORF, or the a′ probe, which is inside the *FUN36* ORF, and (2) the upstream probe b, which is the *Bgl*II fragment shown in Figure 1, or b′, which is internal to the *FUN33* ORF. Hybridization with the a or a′ probe and the b or b′ probe gave the same results, and they will be designated here as probe a or probe b. For studies of breaks located in the *YCR47C/48W* region of chromosome III (Zenvirth *et al.* 1992), the 667-bp *Xba*I/*Eco*RV fragment isolated from plasmid PM5239 was used as a probe (gift from L. Grivell). All probes were labeled by the random priming method according to the manufacturer (Pharmacia, Piscataway, NJ) using 50 μCi of 3000 Ci/mm [α^{32}P]dCTP (Amersham). Hybridization conditions were as specified by Church and Gilbert (1984). The filters were exposed to Amersham Hyperfilms with intensifying screens for 2–7 days or were analyzed with the PhosphorImager system (Molecular Dynamics, Sunnyvale, CA).

For analysis of the processing of DSBs, denatured DNA digests were separated on a 0.8% agarose alkaline gel run in 50 mm NaOH, 1 mm EDTA and blotted to a Genescreen membrane (Dupont-New England Nuclear) using the method of Bishop *et al.* (1992). The DNA was UV cross-linked using the Stratalinker (Stratagene, La Jolla, CA). The exposure was 100 sec at 1200 μJ. Strand-specific ^{32}P-labeled RNA probes were made from pK Bluescript by *in vitro* transcription of cloned DNA (Promega, Madison, WI). A standard transcription protocol with T3 or T7 RNA polymerase and 800 Ci/mm [α^{32}P]UTP (Amersham) was used. These probes are indicated in Figures 1 and 5. The conditions of hybridization and washing were similar to those used in nondenaturing Southern analysis.

Quantification of DSBs: Quantitative estimation of radioactivity on the blots was done by scanning membranes with the SOFI radioimager (Quartz et Silice) or by analyzing an exposed phosphor screen with a PhosphorImager system (Molecular Dynamics) followed by ImageQuant software analysis (Molecular Dynamics). The quantification of DSBs (percentage) is calculated as the percent of radioactivity in both *CYS3* DSB fragment groups relative to the total amount of parental plus DSB fragments (including the *DEP1* fragment, when it was detectable). The quantitations were performed by selecting an exposure time that allows accurate determination of the intensity of the parental band (linear response). Sometimes, however, this means that the signal for the DSB fragment is very weak and very difficult to be quantified reliably. This is particularly the case in *RAD50* strains. Therefore, the exposures that are presented in the figures, which were chosen to best illustrate weak signals, are not always the same as those used for quantitation.

RESULTS

Genetic analysis of meiotic recombination at the *CYS3* locus: The *CYS3* locus, originally called *STR1* (Cherest and Surdin-Kerjan 1992), is located on chromosome I between the *FUN54* (also called *DEP1*) and *FUN36* (Figure 1) ORFs (Ono *et al.* 1992; Barton *et al.* 1993; Ouellette *et al.* 1993). In a previous study of the meiotic segregation pattern of the *str1-1* allele in a *STR1*/

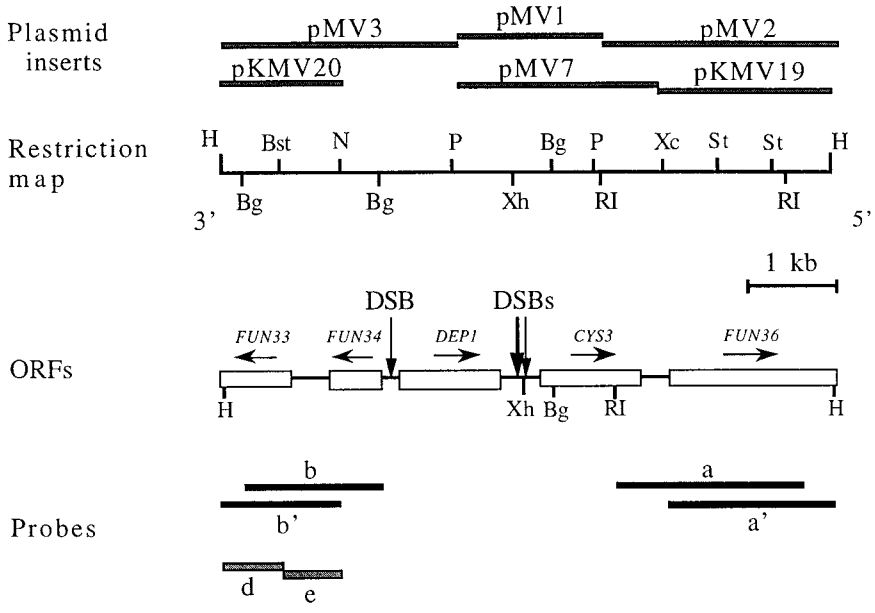

Figure 1.—Physical and functional maps of the *CYS3* region, plasmid inserts, and probes. The name and the relevant insert of the plasmids used in this report are indicated in the upper part of the figure. Restriction sites are as follows: Bg, *Bgl*II; Bst, *Bst*BI; H, *Hin*dIII; N, *Nco*I; P, *Pst*I; RI, *Eco*RI; St, *Sty*I; Xc, *Xca*I; and Xh, *Xho*I. ORFs are mentioned according to Ouellette *et al.* (1993). Horizontal arrows correspond to the direction of transcription. At the bottom, the black bars correspond to double-strand probes, and the gray bars correspond to the single-strand probes. The positions of the meiotic DSB sites are indicated by vertical arrows.

TABLE 1

Yeast strains used in this study

Strain	Genotype
Haploids	
MGD131-102A	*MAT***a** *ura3-52 trp1-289 arg4Δ2060 his3Δ1 ade2*
MGD131-2C	*MATα ura3-52 trp1-289 arg4Δ2060 cyh^R leu2-3,112*
ORT126	*MAT***a** *ura3-52 trp1-289 arg4-Bg his3Δ1 ade2*
ORT118	*MATα ura3-52 trp1-289 arg4-RV cyh^R leu2-3,112*
ORT305	*MATα ura3-52 trp1-289 arg4-RV leu2-3,112 cyh^R rad50S*
ORT311	*MAT***a** *ura3-52 trp1-289 arg4-Bg his3Δ1 ade2 rad50S*
ORT2011	*MATα ura3-52 trp1-289 arg4Δ2060 cyh^R leu2-3,112*
ORT2014	*MATα ura3-52 trp1-289 arg4Δ2060 cyh^R leu2-3,112 cys3-Bg*
ORT2017	*MAT***a** *ura3-52 trp1-289 arg4Δ2060 his3Δ1 ade2 cys3-RI*
ORT2020	*MAT***a** *ura3-52 trp1-289 arg4Δ2060 his3Δ1 ade2 cys3-RI*
ORD1449-20C	*MATα ura3-52 trp1-289 arg4-poly1RV leu2-3,112 his3Δ1*
ORD1450-28B	*MAT***a** *ura3-52 trp1-289 cyh^R arg4-Bg msh2::Tn10LUK7-7 pms1::TRP1 cys3-RI*
ORD1453-13C	*MTA***a** *ura3-52 trp1-289 arg4-Bg cyh^R leu2-3,112 msh2::Tn10LUK7-7 pms1::TRP1 cys3-Bg*
ORD1453-26C	*MATα ura3-52 trp1-289 arg4-Bg leu2-3,112 msh2::Tn10LUK7-7 pms1::TRP1*
ORD1751-70D	*MAT***a** *ura3-52 trp1-289 arg4-poly1Bg cyh^R ade2*
ORD1475-35C	*MAT***a** *ura3-52 trp1-289 arg4-poly1RV ade2 cyh^R his3Δ1 cys3-RI*
ORD1477-13B	*MATα ura3-52 trp1-289 arg4-poly1Bg leu2-3,112 cyh^R cys3-Bg*
ORD1477-40C	*MATα ura3-52 trp1-289 arg4-poly1Bg leu2-3,112 cyh^R cys3-Bg*
ORD2000-231A	*MATα ura3-52 trp1-289 arg4Δ2060 cyh^R leu2-3,112 cys3-Bg*
ORD2000-192A	*MATα ura3-52 trp1-289 arg4Δ2060 cyh^R leu2-3,112 cys3-Bg*
ORD2024-15B	*MAT***a** *ura3-52 trp1-289 arg4Δ2060 cyh^R cys3-Bg,RI*
ORD2024-16B	*MAT***a** *ura3-52 trp1-289 arg4Δ2060 leu2-3,112 cys3-Bg,RI*
ORD2024-29A	*MATα ura3-52 trp1-289 arg4Δ2060 cyh^R leu2-3,112 cys3-Bg*
ORD2024-64C	*MATα ura3-52 trp1-289 arg4Δ2060 cyh^R leu2-3,112 his3Δ1*
ORD2024-71A	*MATα ura3-52 trp1-289 arg4Δ2060 leu2-3,112 ade2 cys3-Bg,RI*
ORD2024-101D	*MATα ura3-52 trp1-289 arg4Δ2060 his3Δ1 ade2 cys3-RI*
ORD2024-107C	*MAT***a** *ura3-52 trp1-289 arg4Δ2060 his3Δ1 ade2 cys3-RI*
ORD2024-108C	*MAT***a** *ura3-52 trp1-289 arg4Δ2060 cyh^R cys3-Bg,RI*
ORD2024-121C	*MAT***a** *ura3-52 trp1-289 arg4Δ2060 cyh^R his3Δ1*
ORD2024-134B	*MAT***a** *ura3-52 trp1-289 arg4Δ2060 his3Δ1 ade2 cys3-Bg,RI*
ORD2024-135B	*MAT***a** *ura3-52 trp1-289 arg4Δ2060 cys3-Bg,RI*
ORD2036-2C	*MAT***a** *ura3-52 trp1-289 arg4Δ2060 his3Δ1 ade2 cys3-RI rad50S*
ORD2039-14B	*MATα ura3-52 trp1-289 arg4Δ2060 cyh^R leu2-3,112 rad50S cys3-Bg*
ORD2043-9B	*MATα ura3-52 trp1-289 arg4-Bg cyh^R ade2 msh2::Tn10LUK7-7 pms1::TRP1 rad50S*
ORD2043-13B	*MAT***a** *ura3-52 trp1-289 arg4-RV cyh^R msh2::Tn10LUK7-7 pms1::TRP1 rad50S*
ORD2052-51B	*MATα ura3-52 trp1-289 arg4-poly1RV leu2-3,112 cys3-RI*
ORD2052-66D	*MAT***a** *ura3-52 trp1-289 ARG4-poly1 his3Δ1 cyh^R ade2 cys3-Bg*
ORD2052-78D	*MAT***a** *ura3-52 trp1-289 ARG4-poly1 his3Δ1 ade2 cys3-RI*
ORD2053-14C	*MATα ura3-52 trp1-289, arg4-poly1RV leu2-3,112 cys3-Bg,RI*
ORD2053-16C	*MAT***a** *ura3-52 trp1-289 arg4-poly1RV his3Δ1 cys3-Bg,RI*
RKY1929	*MATα ura3-52 trp1-289 arg4-Bg cyh^R leu2-3,112 msh2::Tn10LUK7-7 pms1::TRP1*
RKY1935	*MATα ura3-52 trp1-289 arg4-RV cyh^R leu2-3,112 msh2::Tn10LUK7-7 pms1::TRP1*
RKY1939	*MAT***a** *ura3-52 trp1-289 his3Δ1 ade2 msh2::Tn10LUK7-7 pms1::TRP1*
Diploids	
ORD149	ORT118 × ORT126
ORD307	ORT305 × ORT311
ORD1433	ORD2024-15B × ORD2024-64C
ORD1434	ORD2024-16B × ORD2024-64C
ORD1435	ORD2024-108C × ORD2024-64C
ORD1436	ORD2024-135B × ORD2024-64C
ORD1437	ORD2024-71A × ORD2024-121C
ORD1438	ORD2024-134B × MGD131-2C
ORD1442	ORD2024-29A × ORT2017
ORD1443	ORD2024-29A × ORT2020
ORD1444	ORD2024-29A × ORD2024-107C
ORD1450	RKY1935 × ORT2020

(*Continued*)

TABLE 1

(Continued)

Strain	Genotype
ORD1453	RKY1929 × ORD2024-17C
ORD1455	ORD1453-13C × ORD1453-26C
ORD1457	ORD1450-28B × ORD1453-26C
ORD1475	ORD1449-20C × ORD2024-101D
ORD1477	ORD1751-70D × ORD2024-29A
ORD2000	ORT2011 × MGD131-102A
ORD2003	ORT2014 × MGD131-102A
ORD2007	ORT2017 × MGD131-2C
ORD2010	ORT2020 × MGD131-2C
ORD2023	ORD2000-192A × ORT2017
ORD2024	ORD2000-231A × ORT2020
ORD2036	ORT305 × ORT2017
ORD2039	ORT311 × ORD2000-231A
ORD2040	ORD2039-14B × ORD2036-2C
ORD2043	RKY1935 × ORT311
ORD2047	ORD2043-9B × ORD2043-13B
ORD2048	RKY1929 × RKY1939
ORD2049	ORT118 × ORD149-340A
ORD2052	ORD1477-13B × ORD1475-35C
ORD2053	ORD1477-40C × ORD1475-35C
ORD2070	RKY1935 × ORD2052-66D
ORD2072	RKY1935 × ORD2052-78D
ORD3703	ORD2053-16C × ORD2052-51B
ORD3704	ORD2052-66D × ORD2053-14C

str1-1 diploid (a one-point cross), it was reported that NMS (3+:1− and 1+:3− conversion events) occurs at a frequency of 15% (18 events out of 111 tetrads analyzed, Cherest and Surdin-Kerjan 1992).

To confirm that the *CYS3* locus is a hotspot of meiotic gene conversion, we introduced two novel markers into this gene and analyzed the frequency of NMS in strains carrying these alleles. These *CYS3* mutations were constructed *in vitro* by filling in natural restriction enzyme sites, and they are located at positions +154 (*cys3-Bg*) and +808 (*cys3-RI*) with respect to the first nucleotide (A of the ATG) of the *CYS3* coding region (Figure 1). Upon introduction into the wild-type locus by the two-step transplacement procedure (materials and methods) in haploid strains, the *cys3-Bg* and *cys3-RI* mutations, which create +4-bp frameshifts, were found to confer cysteine auxotrophy. *CYS3* mutants can grow on media supplemented with either 0.5 mm cysteine or 0.5 mm glutathione. The genotypes of these yeast strains are listed in Table 1.

The meiotic segregation pattern of these mutations was first examined in diploids heterozygous for a single mutation (one-point cross). *CYS3*/*cys3-Bg* and *CYS3*/*cys3-RI* diploids were sporulated, and unselected tetrads were dissected and analyzed. The results reported in Table 2 show that the *cys3-Bg* marker exhibits a much higher frequency of NMS (28%) than does the *cys3-RI* marker (7%). These values bracket the previous report of 15% found for the *str1-1* allele, which is mutated at an unknown position (Cherest and Surdin-Kerjan 1992). Because the average level of gene conversion found at most loci in yeast is 2–3% (Fogel *et al.* 1981), we conclude that the *CYS3* locus is a hotspot of meiotic gene conversion. The vast majority of conversions involving the *cys3-Bg* and *cys3-RI* markers are 3+:1− and 1+:3− NMS events without a bias in the direction of conversion ($P > 0.05$), and they reflect a single conversion event per meiosis. Among 420 tetrads, four 4+:0− and two 0+:4− tetrads were observed. Their occurrence can result from premeiotic events or from two independent events in which each of two sister chromatids is converted in the same meiosis. No PMS (5+3− or 3+5−) events producing *CYS3*/*cys3* sectored colonies were observed, which is in accordance with previous studies showing that small base pair insertion and deletion mutations give only 3+:1− and 1+:3− conversion events in MMR-proficient strains (Fogel *et al.* 1981; Nicolas *et al.* 1989; Detloff *et al.* 1992).

To further characterize recombination events at the *CYS3* locus, we then studied the segregation of the *cys3-Bg* and *cys3-RI* markers in two-point crosses, with these markers in the *trans* (*Bg* +/+ *RI*) or *cis* (*Bg RI*/+ +) configurations. Unselected tetrad analysis of heteroallelic diploids allows various classes of segregation events to be distinguished: single-site conversions, simultaneous conversion of both sites in one direction (coconversion), reciprocal exchanges, and complex events involving one or both markers on more than two chromatids

TABLE 2

Tetrad analysis of recombination events at the *CYS3* locus in wild-type strains

Cross	Allele	*N*	Single-site conversion 3+:1−	Single-site conversion 1+:3−	Coconversion 1*cys3-RI*: 3*cys3-Bg*	Coconversion 1*cys3-Bg*: 3*cys3-RI*	RE	Other events	%
NMS events observed in a one-point cross[a]									
Bg + / + +	*cys3-Bg*	420	42	64			0	6	28
Bg RI / + *RI*	*cys3-Bg*	154	27	15			0	0	27
+ *RI* / + +	*cys3-RI*	661	23	25			0	0	7
Bg RI / *Bg* +	*cys3-RI*	146	7	11			0	0	12
Results of two-point crosses[b]									
Bg + / + *RI*	*cys3-Bg*	529	49	62	38 (82)	44	5	40	44
	cys3-RI		11	9				33	26
Bg RI / + +	*cys3-Bg*	295	14	20	26 (48)	22	1	12	32
	cys3-RI		1	4				9	21

The total number of coconversions is indicated between parentheses. The genotypic compositions of the exceptional tetrads obtained from the two-point crosses are indicated in the Figure 2. *N*, number of tetrads with four viable spores; RE, reciprocal exchanges, %, percentage of tetrads exhibiting NMS with respect to *N*.

[a]For the *cys3-Bg* (ORD2000 and ORD2003) or the *cys3-RI* mutations (ORD2007, ORD2009, and ORD2010). Other events in the *Bg* +/++ diploids are 4 (4+:0*Bg*) and 2 (0+:4*Bg*). Results from diploids auxotrophic for cysteine are shown as a control: *Bg RI*/*Bg*+ (Ord3704) and *Bg RI*/+*RI* (ORD3703).

[b]The analyses were performed with the *cys3-Bg* and *cys3-RI* markers in the *trans*-configuration (*Bg* +/+ *RI*, data obtained from ORD2023, ORD2024, ORD1442, ORD1443, ORD2052, and ORD2053 diploids) or in the *cis*-configuration (*Bg RI*/++, data obtained from ORD1433–1438 diploids).

per meiosis. Our analysis of the results is shown in Table 2, and the genotypic composition of exceptional tetrads is reported in Figure 2. In heteroallelic diploids, spore viability is ~70%, comparable to that observed in one-point crosses. For the *trans* configuration, the frequency of tetrads exhibiting NMS is very high, as much as 48% (256/529). Among these, NMS events involving the *cys3-Bg* marker represent 91% (233/256) of the recombinant tetrads, and those involving the *cys3-RI* marker represent 52% (135/256). Conversions of the *cys3-Bg* marker alone represent 48% (111/233) of the cases of conversion at this site, and those of the *cys3-RI* marker alone are 15% (20/135) of the events involving this site. Coconversions are frequent (32%, 82/256), and numerous complex events (17%, 43/256) also occur. We observed that numerous tetrads noticeably exhibited 4+:0− and 0+:4− segregation for either of the two markers, indicating that simultaneous conversion of the sister chromatids at one site is frequent, but that conversion at both sites is less common (3/43 complex tetrads). Reciprocal exchanges are rare (2%, 5/261 recombinant tetrads). The surprising aspect of these data is the higher overall NMS frequency of either marker when both are present, as compared to the NMS frequency of either marker alone. In absolute frequencies, the *cys3-Bg* marker exhibits 44% NMS (233/529) instead of 28%, as seen in one-point crosses, and the *cys3-RI* marker exhibits 26% (135/529), compared to 7%.

The results obtained with the two markers in the *cis* configuration also show that tetrads exhibiting NMS are frequent (34%, see Table 2 and Figure 2). Most events involve NMS of either marker; 39% of recombinant tetrads are single-site conversions. Most involve the *cys3-Bg* marker (34/39) and, less frequently, the *cys3-RI* marker (5/39). The other recombinant tetrads correspond to 48% of coconversion, 12% complex events, and 1% reciprocal exchanges. NMS events involving the *cys3-Bg* marker therefore represent 32% (94/295) of total meioses, a frequency slightly higher than that observed for one-point crosses ($P > 0.05$). This value is lower ($P < 0.01$) than that found for the *trans*-heteroallelic diploids (44%); in this case, NMS events involving

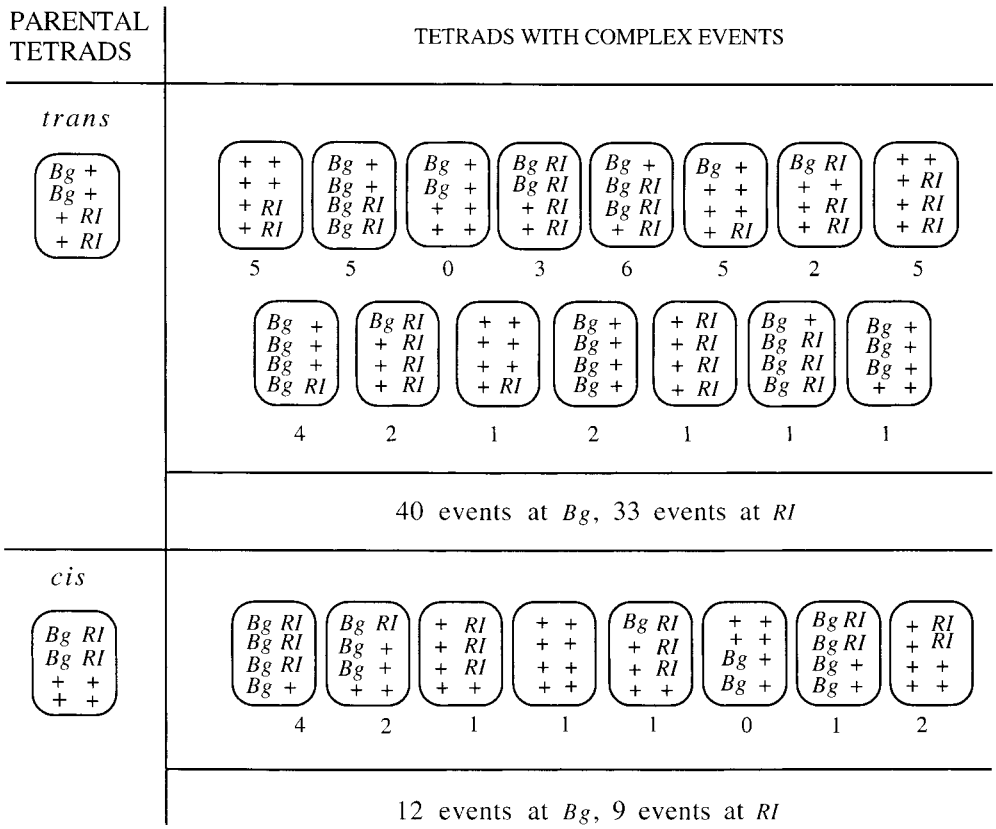

Figure 2.—Genotypic composition of exceptional tetrads in two-point crosses in which the *cys3-Bg* and *cys3-RI* markers are in the *trans*-position (upper part) or *cis*-position (bottom part). In our analysis, the numbers of tetrads with four viable spores were 519 and 295 for the *trans*- and *cis*-configurations, respectively. The number of tetrads of each genotype is indicated under each tetrad.

the *cys3-RI* marker represent 21% (62/295) of total meioses compared to 26% for the *trans*-configuration. Tetrad analysis of gene conversion events in a diploid heterollelic at both *ARG4* (*arg4-RV* +/+ *arg4-Bg*) and *CYS3* (*cys3-Bg* +/+ *cys3-RI*) indicates that the increase of NMS at *CYS3* is not accompanied by a similar enhancement of NMS at the *ARG4* locus, which is located on a different chromosome (data not shown).

To test if cysteine auxotrophy affects the level of NMS events, we examined diploids ORD3703 (+ *RI*/*Bg RI*) and ORD3704 (*Bg* +/*Bg RI*), which are heterozygous for a single marker but auxotrophic for cysteine (see Table 1). We observed (Table 2) that the *cys3-Bg* marker exhibits the same frequency of gene conversion (27%) as that measured from a diploid cysteine prototroph in a one-point cross ($P = 0.88$). In the case of the *cys3-RI* marker, the frequency of gene conversion is slightly but significantly increased (12% instead of 7%; $P = 0.04$). These results indicate that the enhanced NMS frequency of the *cys3-RI* marker observed in two-point crosses could be partially related to cysteine auxotrophy. Further analysis of this unusual marker effect is presented in discussion.

Genetic studies in *msh2 pms1* strains: At the *ARG4* and *HIS4* loci, Alani *et al.* (1994) found that the 5′–3′ conversion gradient is relieved in *msh2*, *pms1*, and *msh2 pms1* strains because of increased NMS frequencies of markers located at the 3′ end of the locus. In one-point crosses, we examined the effect of *msh2 pms1* mutations on NMS in strains with the *cys3-Bg* or *cys3-RI* alleles (Table 3). Diploids (ORD1455 and ORD1457) were sporulated after minimal growth to avoid the accumulation of lethal mutations (materials and methods). Spore viability ranged from 50 to 70%. The frequency of NMS involving the *cys3-Bg* marker in the MMR-deficient background was 18%, and that involving the *cys3-RI* marker was 21%. In the case of the *cys3-Bg* marker, the difference between the mutant (18%) and the wild-type strain (28%) is modest but significant ($P = 0.034$). For the *cys3-RI* marker, the frequency of NMS events is very significantly ($P < 0.005$) enhanced in MMR-deficient strains. As expected for MMR mutants, *msh2 pms1* mutations lead to the appearance of PMS (5+:3−, 3+:5−, aberrant 5+:3−, and aberrant 4+:4−) at the expense of simple gene conversion events (6+:2− and 2+:6− segregation). These PMS events are indicative of the formation of heteroduplex DNA at *CYS3* and of inefficient MMR of these 4-bp insertion mutations. The frequency of PMS among the aberrant events is 60% (18/30) for the *cys3-Bg* marker and 81% (21/26) for the *cys3-RI* marker. We note that 40% of the NMS events involving the *cys3-Bg* marker and 19% at the *cys3-RI* marker are still simple gene conversions, suggesting either that residual MMR activity persists in the absence of the Msh2 and Pms1 proteins, or that these events result from the repair of a double-strand gap (Szostak *et al.* 1983). In the *msh2 pms1* strain, this residual gene conversion frequency of the *cys3-Bg* marker (7%) is sig-

TABLE 3

Tetrad analysis of recombination events at the *cys3-Bg* and *cys3-RI* markers in homozygous *msh2 pms1* diploids

Cross	Alleles	*N*	Conversions		PMS				
			6+:2−	2+:6−	5+:3−	3+:5−	Ab 4+:4−	Others	%
Bg + / + +	*cys3-Bg*	164	10	2	4	11	1	2	18
+ *RI* / + +	*cys3-RI*	126	4	1	12	7	1	1	21

Strains are ORD1455 and ORD1457, respectively. The NMS events were categorized into those that displayed gene conversion (6+:2−, 2+:6−, same as 3+:1− and 1+:3− in Table 2) and those that displayed sectored colony reflecting PMS (5+:3−, 3+:5−, Ab 4+:4−). "Others" are in the ORD1455 (*Bg* +/++) diploid (+/+; +/−; +/−; +/−) and in the ORD1457 diploid (+ *RI*/++) (+/−; −/−; −/−; −/−).

N, number of tetrads with four viable spores; %, percentage of tetrads exhibiting NMS with respect to *N*.

nificantly different from that observed in the wild-type strain (27%; $P < 0.001$). In contrast, conversion of the *cys3-RI* marker is not significantly modified (7 and 4%, for wild-type and the *msh2 pms1* strains, respectively; $P = 0.17$). These results will be compared with those described for *ARG4* and *HIS4* (Alani *et al.* 1994) in discussion.

Meiotic DSBs in the *CYS3* region: DSBs can be detected either as transient DNA fragments of heterogeneous length in wild-type *RAD50* diploid strains (Sun *et al.* 1989) or as discrete bands that accumulate in diploids homozygous for the *rad50S* mutation (Alani *et al.* 1990). This mutation has made it possible to map DSB sites and to quantify the extent of breakage at these sites. We examined the formation of meiotic DSBs near *CYS3* in *rad50S* strains by Southern blot analysis. In addition to the parental fragment (6716 bp), the a and b probes hybridize to two bands of lower molecular weight which are seen only in DNA from meiotic cells (Figure 3A). These fragments, as measured in several independent experiments, constitute 8 ± 2 % of the total DNA molecules hybridizing to the probe. The two DSB regions map in the 5′ intergenic region of the *CYS3* gene. The weaker "proximal" DSB is located around position −160 with respect to the *CYS3* ORF, whereas the stronger band ("distal") is located around position −270. Distal DSBs are two- to threefold more frequent than proximal DSBs. A 4.8-kb meiosis-specific DSB fragment can also be seen in Figure 3. This represents a weak DSB site located between *FUN34* and *DEP1* (Figure 1).

The genetic results presented above show that the frequency of NMS at *CYS3* is about twofold greater in a *trans*-heteroallelic diploid than in a diploid containing only one of the two mutant alleles. To test whether heterozygosities near the DSB sites affect the frequency of DSB formation, we compared DSB levels in *rad50S* diploids homozygous for the wild-type *CYS3* allele (ORD307) or heteroallelic at *CYS3* (ORD2040). As a control, we also examined DSB formation at the *YCR47C/48W* locus on chromosome III (Zenvirth *et al.* 1992; Goldway *et al.* 1993; Baudat and Nicolas 1997). Figure 3B shows Southern blot analysis of DSB formation at *CYS3* (top panels) or at *YCR47C/48W* (bottom panels) in a wild-type diploid (left panels) or a diploid heteroallelic at *CYS3* (right panels). A comparison of the kinetics of formation of DSBs in these strains (Figure 3B) shows that the *CYS3* heteroallelic diploid exhibits a 2-hr delay in DSB formation at both loci. It indicates that this delay does not result from heterozygosity at the *CYS3* locus, but, very likely, that the *CYS3* heteroallelic strain has a different timing for entry or progression into meiotic prophase. At $t = 24$ hr, the amount of DSBs formed at *CYS3* reaches a value of 8.5%, which is similar to that observed in a *CYS3/CYS3* strain (8 ± 2%, Figure 3B). The position of the DSBs is the same as that in wild-type strains (Figure 3B). To verify that the level of DSBs in the *cys3-Bg/cys3-RI* diploid is maximal by 24 hr, we performed an additional experiment that included 32- and 40-hr time points (Figure 3C). The level of DSBs was maximal at 24 hr, whereas it reached a plateau at $t = 12$ hr in the *CYS3/CYS3* diploid. A similar delay was observed in *RAD50* strains in which the DSBs are transient (data not shown). This delay was observed at both loci (*CYS3* and *YCR47C/48W*), and it could originate from metabolic defects resulting from the absence of functional Cys3p, which might not be fully compensated for by the addition of glutathione. Taken together, these data allow us to conclude that the presence of heterozygous markers in the *CYS3* coding region does not affect the frequency or distribution of DSBs in this region.

The formation of meiotic DSBs at *CYS3* in the *RAD50* strain background was studied in the diploids ORD149 or ORD2049 (Table 1). With both probes a and b (Figure 4), we observed the appearance of smeared DSB fragments, indicating that both ends of the *CYS3* meio-

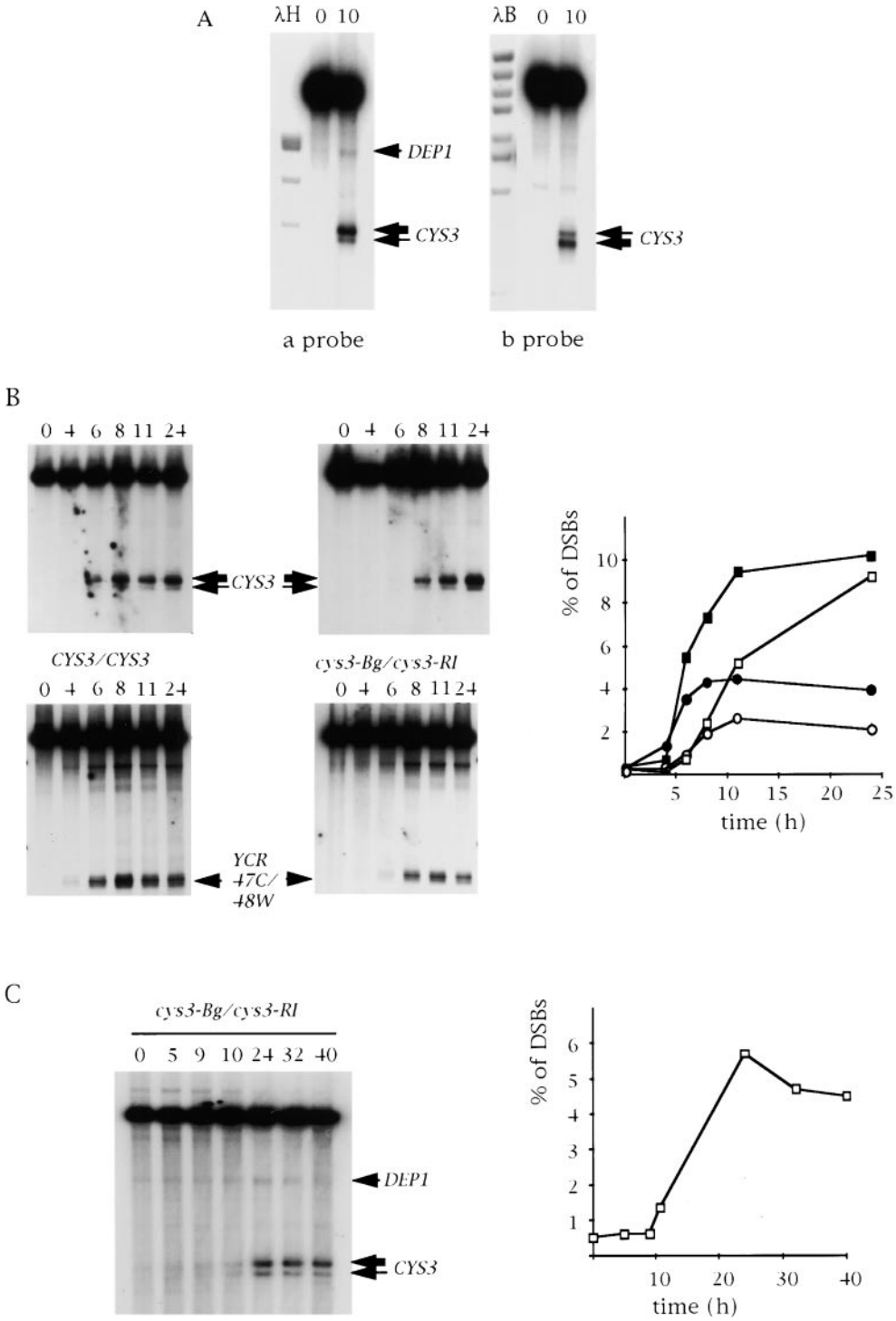

Figure 3.—Detection, mapping, and quantification of meiotic DSBs at the *CYS3* recombination hotspot in *rad50S* strains. Meiotic cells are harvested from sporulation medium at various times during sporulation ($t = 0$–24 hr). DNA from the samples is purified; 1–2 μg of DNA is *Hin*dIII digested and analyzed by Southern blot. Random-primed-labeled a and b probes are as indicated in Figure 1. The *Hin*dIII parental fragment (6710 bp) is at the top of each autoradiogram. In the case of the *CYS3* locus, the DSBs are indicated with horizontal arrows of unequal size representing the relative intensity of the two bands. The quantification of DSBs (percentage of DSBs) is calculated as the percentage of radioactivity in both *CYS3* DSB fragment groups relative to the total amount of parental plus DSB fragments (including the *DEP1* fragment when it was detectable). (A) Detection and mapping of meiotic *CYS3* DSBs, probing with the a (left part) or b (right part) fragment. Molecular weight markers are λ/*Hin*dIII (λH) and λ/*Bst*EII (λB) digestions. (B) Comparison of DSB formation between homoallelic ORD307 (*CYS3*/*CYS3* on the left part) and heteroallelic ORD2040 (*cys3-Bg*/*cys3-RI* on the middle part) at the *CYS3* (top) or at *YCR47C*/*48W* (bottom) loci. For both loci, genomic DNA was digested by *Hin*dIII. In the case of *CYS3*, the probe was a, as indicated in Figure 1. In the case of the *YCR47C/48W* locus, an *Xba*I/*Eco*RV fragment containing a *YCR47C* ORF part was labeled as a probe for this region. Other legends are as described in A. The quantification and kinetics of the DSB accumulation at the *CYS3* (squares) and the *YSC47C*/*48W* (circles) loci in ORD307 (filled squares or circles) or in ORD2040 (open squares or circles) is shown on the right. (C) Extended time course in the *cys3-Bg*/*cys3-RI* heteroallelic strain (ORD2040); the quantification and kinetics of the *CYS3* DSBs are shown in the right part.

sis-specific breaks were resected, as has been found for the *ARG4* (Sun *et al.* 1991) and *HIS4-LEU2* loci (Cao *et al.* 1990). The smeared products appear as diffuse signals with a bandwidth of 200–300 bp. The bands in the *RAD50* sample are of lower molecular weight than the corresponding bands in the *rad50S* sample. The kinetics and the quantification of band intensities are diagrammed in Figure 4. DSB fragments corresponding to both sides of the break appear with similar kinetics. The smears appear at $\sim t = 6$ hr after transfer into sporulation

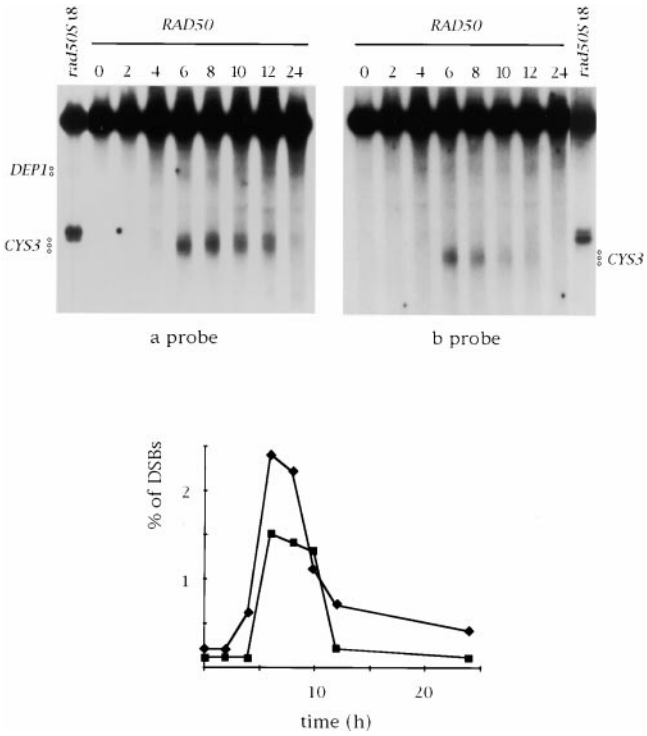

Figure 4.—Detection of meiotic DSBs at the *CYS3* recombination hotspot in the *RAD50* strain (ORD149). The DNA was digested with *Hin*dIII and blotted as described previously. Each membrane was hybridized with the a or b probe (see Figure 1). A *Hin*dIII digestion of DNA from cells harvested at $t = 8$ hr from the *rad50S* isogenic strain ORD307 ($t = 8$ hr) was added as a control in each blot. The vertical open circles indicate the smear corresponding to the transient DSB fragments. A quantitative analysis of labeling in the smears is shown, using the a (diamonds) or the b (squares) probe. The graph indicates the percentage of the labeling in the DSB smear (percent of DSBs) plotted over time in sporulation medium. The percentage is calculated as explained in Figure 3.

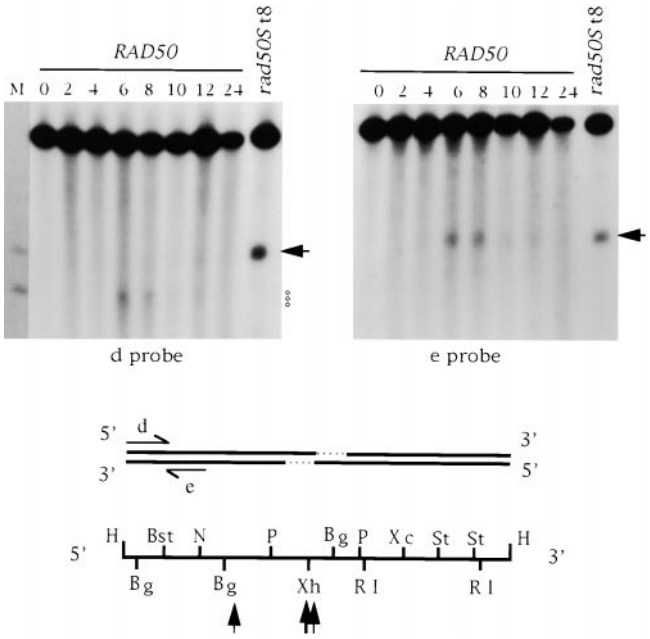

Figure 5.—Analysis of individual component strands of DSB fragments in the *RAD50* strain (ORD149). DNA was digested with *Hin*dIII, fractionated on an alkaline gel, and blotted onto a Genescreen membrane. (Top) Southern analysis using single-stranded d or e riboprobes to detect each strand that has its 3′ or 5′ ends at the DSB site. The *Hin*dIII-digested DNA from strain ORD307 (*rad50S*) at $t = 8$ hr is shown as a control. Molecular weight markers in the line M were generated by double digestion of genomic DNA with *Hin*dIII/*Xho*I (3344 bp) or *Hin*dIII/*Bst*EII (2789 bp). The horizontal arrows indicate the DSB product from the *rad50S* strain. (Bottom) Partial restriction map of the *Hin*dIII parental fragment; d and e strand-specific RNA probes and their orientation are schematized by horizontal arrows. The probe d has the sequence of the top strand, the e probe has that of the bottom strand. Other legends are as described in Figures 1–3.

medium, they reach maximal intensity at $\sim t = 8$ hr, and then disappear between $t = 10$ and $t = 24$ hr, at which time ascospores are formed.

To test whether meiotic DSBs at *CYS3* are resected as they are at the *ARG4* (Sun *et al.* 1991) and *HIS4-LEU2* loci (Bishop *et al.* 1992), DSB fragments were resolved on alkaline denaturing gels and hybridized to single-strand-specific riboprobes (Figure 5). These probes are complementary either to the top strand (e probe) or the bottom strand (d probe), and they are specific to the 5′ side of the *CYS3* locus (Figure 1). With the e probe, we observed a break-specific band of about the same length as that found in the *rad50S* background, indicating that this strand is not resected. This strand has its 3′ extremity at the DSB site (the 3′ end). The d probe, which corresponds to the complementary strand (the 5′ end), hybridizes to fragments of heterogeneous length from $t = 4$ to $t = 12$ hr. This smear is ~200–300 nucleotides wide, and the fragments at the top of the smear are ~400 bases shorter than the fragment found in the *rad50S* strain. We address this finding in discussion. Two other single-strand probes (f and g) were also used to probe the proximal side of the *CYS3* DSBs (Figure 1). The 3′ end was also observed as an unresected fragment, and the 5′ end was observed as a faint smear (data not shown).

DSBs in *msh2 pms1* strains: To identify the recombination intermediate(s) on which the MMR proteins Msh2p and Pms1p act, we studied the processing of DSBs in homozygous *msh2 pms1* strains. To rule out the possibility that the absence of Msh2p and Pms1p affects the formation of DSBs, we first examined meiotic DSBs in *msh2 pms1 rad50S* diploids (Figure 6). We observed that both *CYS3*-proximal and -distal DSBs are formed, and that no other DSB sites appear either in the *CYS3* coding region or further downstream (data not shown). A quantification of *CYS3* DSBs in each strain is shown in Figure 6. DSBs accumulate as unresected fragments at the same level in a *msh2 pms1 rad50S* mutant strain (7 ± 1.5%) as they do in *MSH2 PMS1 rad50S* strains (8 ± 2%). The ratios of the frequencies of the distal and proximal DSBs remain similar for both strains during the entire time

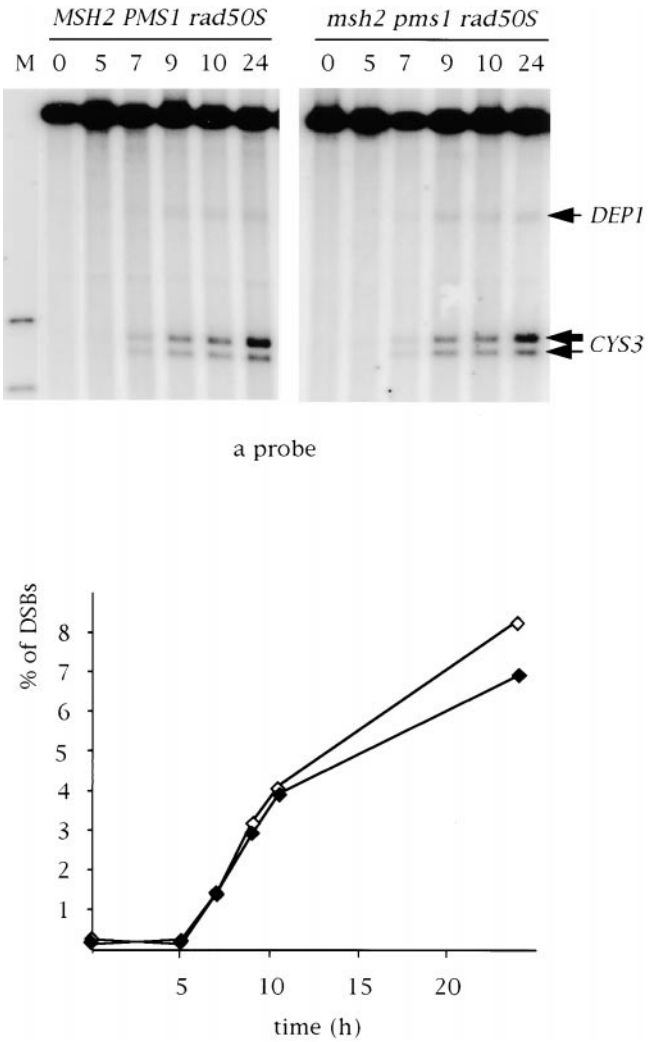

Figure 6.—Detection and quantification of meiotic DSBs at the *CYS3* locus in wild-type and *msh2 pms1* strains in the *rad50S* background. The DNA from the *rad50S* (ORD307) or the *msh2 pms1 rad50S* strain (ORD2047) was digested with *Hin*dIII and revealed with the a probe. M, mix of *Hin*dIII/*Xho*I plus *Hin*dIII/*Bgl*II double-digested genomic DNA used as ladders. The kinetic of accumulation of the *CYS3* DSBs during the time course is shown on the graph: ORD307 (solid diamonds) and ORD2047 (open diamonds). The percentage of DSBs at *CYS3* is calculated as explained in Figure 3.

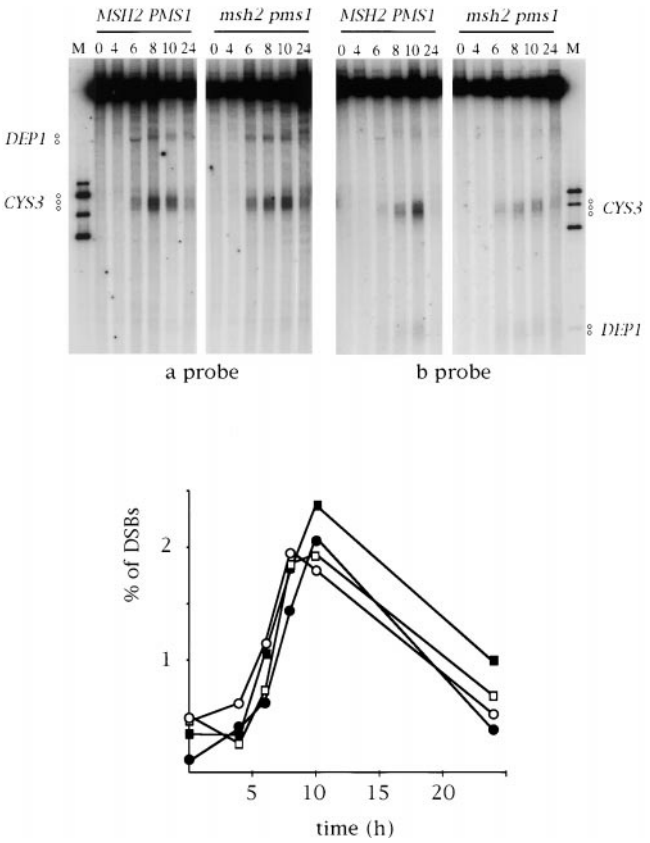

Figure 7.—Analysis of *CYS3* DSBs in the wild-type (ORD-2049) or *msh2 pms1* strain (ORD2048). DNA was digested with *Hin*dIII and probed from each side of the *CYS3* DSBs (a or b probe). M is a mix of *Hin*dIII/*Xho*I, *Hin*dIII/*Sma*I, *Hin*dIII/*Pst*I, and *Hin*dIII/*Bgl*II. The molecular weights of these fragments are 3587, 3367, 3048, and 2520 bp, revealed with the a probe, and 3344, 3123, 2789, 2612, and 1274 bp, revealed with the b probe. The vertical open circles indicate the smear corresponding to the DSB fragments at the *CYS3* or *DEP1* locus. The graph shows a quantitative analysis of the diagnostic fragments from DSBs at the *CYS3* locus. The percentage of the labeling in the DSB smears on either side of the DSBs with the a (squares) or b (circles) probe is plotted over time in sporulation medium. Solid symbols, wild-type strain; open symbols, *msh2 pms1* strain.

course. We then examined the formation of meiotic DSBs in *msh2 pms1 RAD50* cells (ORD2048) with respect to a wild-type strain (ORD2049). The percentage of sporulation (dyads, triads, and tetrads) at 72 hr after the induction of meiosis was similar in both strains (77% in ORD2049, 70% in ORD2048). Figure 7 shows a Southern blot analysis of time course experiments in which both sides of the DSB region were probed (probes a and b, as illustrated in Figure 1) for each strain. In both strains, DSBs are visualized as smeared and transient signals indicative of the formation of resected DSB fragments. The kinetics of signal appearance and disappearance are similar in both strains (Figure 7). At the peak of their accumulation, the frequency of these transient diagnostic fragments is identical (2.0 ± 0.5%) in both *msh2 pms1* and wild-type strains. Altogether, this physical analysis shows that the *msh2 pms1* mutations do not affect the formation of meiotic DSBs.

DISCUSSION

This article reports on the genetic and molecular characterization of recombination events at the *CYS3* locus, a hotspot of meiotic gene conversion. In the wild-type strain background, the meiotic segregation analysis of two new frameshift mutations of *CYS3* revealed high levels of gene conversion. The *cys3-Bg* marker located at the 5′ end of the gene exhibits a particularly high level of gene conversion (27%). This value is about

three- to fourfold higher than that of a similarly positioned mutation in the *ARG4* coding region (7% for the *arg4-RV* marker), and it is even greater than the peak (17%) of gene conversion observed for *ARG4* (Schultes *et al.* 1990). The difference in the absolute levels of gene conversion frequencies between *CYS3* and *ARG4* can be explained by a higher level of DSB formation in the *CYS3* promoter, which is 8 ± 2%, *i.e.*, threefold, higher than at *ARG4* (2–3%). The frequency of DSB formation at *CYS3* is one of the highest found in a wild-type chromosomal segment (Baudat and Nicolas 1997). Our *cys3-RI* marker, located towards the 3′ end of the *CYS3* coding region, exhibits a lower frequency of gene conversion (7%), which is likely to result from a 5′–3′ decreasing gradient of conversion in *CYS3*, similar to that of the well-characterized *ARG4* (Fogel *et al.* 1981; Nicolas *et al.* 1989) and *HIS4* (Detloff *et al.* 1992) hotspots. This conclusion is based on the study of only two markers. However, it is reinforced by our observation that the difference in conversion frequencies of the *cys3-Bg* and *cys3-RI* markers is relieved in MMR mutants (*msh2 pms1*), as observed previously for the *ARG4* and *HIS4* conversion gradients (Alani *et al.* 1994). Further discussion of this phenomenon in the context of our study of meiotic DSBs is presented below. We conclude that *CYS3* is a very strong hotspot of meiotic gene conversion, with a 5′–3′ gradient that resembles that of *ARG4* (Fogel *et al.* 1981; Nicolas *et al.* 1989), *DED81* (Schultes and Szostak 1990), and *HIS4* (Detloff *et al.* 1992), but not that of *HIS2*, where the gradient is of opposite polarity (3′–5′, Malone *et al.* 1992).

Meiotic recombination hotspots in *S. cerevisiae* are characterized by the formation of transient DNA DSBs during meiotic prophase. Studies in which *cis*-acting sequences were deleted, or heterologous sequences were inserted, or in which the effects of *trans*-acting factors were assessed have demonstrated that these DSBs are an early step in the initiation of recombination (reviewed in Nicolas and Petes 1994; Lichten and Goldman 1995). In the presence of the *rad50S* mutation, in which DSBs form but are not processed (Alani *et al.* 1990), two discrete DSB regions can be detected in the 5′ region of the *CYS3* locus. The two regions are ~150 ± 50 bp apart and undergo breakage to different extents: the distal DSBs are about two- to threefold more frequent than the proximal DSBs. No significant variation in the ratio of DSB formation at these two sites was observed during the course of meiosis. These results are in agreement with the higher-resolution mapping of DSBs at *CYS3* (de Massy *et al.* 1995). Two DSB regions are also found at the DED82/DED81 divergent promoters (Wu and Lichten 1994), but they are not observed at the *ARG4* locus or at *HIS4* (Xu and Petes 1996).

Interestingly, the two regions of DSB formation upstream of *CYS3* are also micrococcal nuclease-hypersensitive sites (Ohta *et al.* 1994). The sensitivity of these sites increases two- to fourfold before the appearance of meiotic DSBs and recombination products (4 hr after transferring cells into sporulation medium). Meiotic hypersensitivity to deoxyribonuclease I has also been observed in the *YCR47C/48W* region and at the *ARG4* locus by Wu and Lichten (1994). A meiosis-specific change in chromatin structure has also been detected in the wild-type strains at the *HIS4* hotspot (Fan and Petes 1996). The relationship between these alterations in chromatin structure and the transcriptional state of the adjacent gene remains unclear, and it varies among recombination hotspots (Fan *et al.* 1995). In the case of *CYS3*, we have observed a threefold increase in the steady-state level of *CYS3* mRNA 1 hr after the shift into sporulation medium (M. Vedel, unpublished data), which is before the increase in sensitivity to micrococcal nuclease. RNA polymerase II holoenzyme has been shown to contain SWI/SNF regulators, which are involved in chromatin remodeling (Wilson *et al.* 1996). The increased level of steady-state *CYS3* mRNA may reflect an activation process that could act at the level of chromatin to facilitate the accessibility of the region to the Spo11p nuclease, which is responsible for DSB formation (Bergerat *et al.* 1997; Keeney *et al.* 1997).

At the *ARG4* locus, with few exceptions (*e.g.*, ΔHA-315), there is a good correlation between DSB levels and the frequencies of NMS, suggesting that most recombination events at this locus are initiated by meiotic DSBs, and that these breaks are repaired by copying from the homologous chromosome (de Massy and Nicolas 1993). These data are consistent with the observation that double Holliday junctions (a subsequent recombination intermediate) preferentially form between homologs rather than between sister chromatids (Schwacha and Kleckner 1995). In the *CYS3* region, DSBs represent a 6–10% cleavage per meiotic DNA molecule. Assuming that the two sister chromatids of each homolog are equally prone to DSB formation, this is approximately what is expected if most NMS events (27–28% involving the *cys3-Bg* marker, which is ~310 or 420 bp from the DSB sites) are initiated by adjacent DSBs. We observe in one-point crosses a high level of conversion at the distant *cys3-RI* site (7–12%), and in *cis*- and *trans*-two-point crosses, there is a high proportion of coconversion events involving both *cys3-Bg* and *cys3-RI* (92 and 83% of NMS tetrads, respectively). These results strongly suggest that conversion at the 3′ end of the *CYS3* locus also depends on the initiating DSBs located in the intergenic promoter region of *CYS3*. In this respect, recombination at the *CYS3* locus is mechanistically similar to that at *ARG4* (Sun *et al.* 1989), with prominent DSB-induced conversion events occurring nearby.

In several instances, "marker effects" have been reported in which a heterozygous state decreases the frequencies of conversion of adjacent markers by affecting the initiation of recombination or the processing of heteroduplex intermediates (reviewed in Nicolas and

Rossignol 1989; Keeney and Kleckner 1996; Rocco and Nicolas 1996). As another example, in an inverted repeat assay system, a single mismatch has been found to modify the rate of mitotic recombination between otherwise identical sequences in MMR-competent cells (Datta *et al.* 1997). In this case, the incidence of crossing over was reduced approximately fourfold. Marker effects increasing the gene conversion frequencies of adjacent markers were also found for the *buff-YS17* mutation in *Sordaria brevicollis* (Whitehouse 1982) and in the *ade6-M26* mutation in *Schizosaccharomyces pombe* (Zahn-Zabal and Kohli 1996 and references within). In both cases, these mutations are likely to stimulate the initiation of recombination as they undergo a higher level of NMS than do nearby markers, with respect to what is measured in one-point crosses. The result of our genetic analysis at *CYS3* showing that gene conversion frequencies in two-point crosses are higher than in one-point crosses, especially in the case of the *trans*-heteroallelic (*RI* + / + *Bg*) diploid ($P < 0.001$), was therefore unexpected. It was not observed in the extensive one-point and multipoint analyses of NMS frequencies at the *ARG4* locus (Fogel *et al.* 1971). Three nonexclusive hypotheses may explain the significant increase in conversion frequencies involving the *cys3-Bg* and *cys3-RI* markers when both are present. First, the cysteine auxotrophy of diploids seems to slightly enhance the NMS frequency of only the *cys3-RI* marker, which cannot explain the observed marker effect. The second possibility is that DSB formation is stimulated. To test this hypothesis, we examined the formation of meiotic DSBs in the absence of heterozygosities (*CYS3*/*CYS3*) and in the heteroallelic diploid (*cys3-Bg*/*cys3-RI*). In the *rad50S* background, both strains display a similar DSB frequency in the *CYS3* promoter region. Additional DSBs could have resulted from an interaction between homologs before DSB formation (Keeney and Kleckner 1996; Rocco and Nicolas 1996). Our physical examination of the pattern of DNA fragments in the *CYS3* region or in adjacent regions during meiosis did not reveal any evidence of such an event. We conclude that the presence of both markers in the *CYS3* coding region probably does not affect the formation of initiating DSBs. The third and more probable hypothesis is that this marker effect results from changes in the processing of the recombination intermediates at a stage after DSB formation. The classes of tetrads obtained from the *trans*- and *cis*-heteroallelic diploids, presented in Figure 2, define two prominent categories of events. First, we measure a high level of coconversion, which contributes to the overall increase in NMS. The *cys3-Bg* and the *cys3-RI* markers are ~400 and 1000 bp distant from the DSBs, respectively. In *S. cerevisiae*, the average meiotic gene conversion tract length has been estimated at 1.5–3.7 kb, depending on the locus (Detloff and Petes 1992). Our results indicate that the majority of the aberrant events involving the 3′ marker could be the result of a heteroduplex that extends through the 5′ end of the *CYS3* gene. They also suggest that the presence of heterozygosity may influence the extent of heteroduplex formation so that both markers are more likely to be involved without a change in the direction of the mismatch repair parameters. Second, we detect numerous complex events involving more than two chromatids per meiosis. The existence of these exceptional tetrads suggests that the presence of two heterozygous markers on the same tract of heteroduplex DNA might initiate a second round of recombination events promoted by MMR, as proposed by Hastings (1984). Secondary DNA lesions, such as DSBs and gaps created by converging excision repair processes operating on opposite strands of the same heteroduplex intermediate, could then be repaired by interaction of the affected chromatid with its intact sister or nonsister chromatids to yield three or four recombinant products per meiosis. Another "marker effect" (*i.e.*, an increase in nonreciprocal recombination events) has been observed upon introduction of nine heterozygosities located between an artificially created nontandem duplication of the *MAT* locus in *S. cerevisiae* (Borts and Haber 1987).

The high frequency of DSB formation at the *CYS3* locus allowed us to study the processing of the broken ends in an isogenic *RAD50* strain. As described for the *ARG4* locus (Sun *et al.* 1991) and the *HIS4-LEU2* construct (Cao *et al.* 1990), we observed smeared DSB fragments corresponding to processing intermediates. We used alkaline gels and strand-specific probes to follow the processing of the *CYS3* DSBs and observed the production of 3′ overhanging tails on either side of the DSBs. In our experimental conditions, these tails are 400–700 nt long at *CYS3*, with a constant heterogeneity of ~200–300 nt. In the case of the *ARG4* locus, Sun *et al.* (1989) observed an 800-nt 3′ overhanging tail with a gradient of resection. The analysis by Sun *et al.* (1989) was performed with an SK1 strain in which the *ARG4* region was carried on a single copy plasmid; they used a nondenaturing Southern blot procedure to examine the DSB fragments. Our results with *CYS3* are more similar to those reported by Bishop *et al.* (1992) for the *HIS4-LEU2* hotspot. Using alkaline gels, they determined that in the SK1 background, the 5′ strands are always at least ~600 nt shorter than the 3′ strands. At *CYS3*, we observed that the 5′ strand is at least 400 nt shorter than the 3′ strand. Consequently, the *cys3-Bg* marker, located ~400 bp from the DSBs, is included in the region of single-strand resection, which could explain its high frequency of gene conversion. The mechanism and the protein(s) that create the single-strand tail and control its length remain to be discovered (Keeney *et al.* 1997).

Finally, an important result of our characterization of the *CYS3* hotspot of meiotic gene conversion is a confirmation that the MMR genes are involved in determining the frequency of meiotic gene conversion, as

reported by Alani *et al.* (1994). At the *CYS3* locus, we observed in the *msh2 pms1* mutant strains an important increase of NMS frequency at the *cys3-RI* marker (in more than 25% of the meioses), while the NMS frequency at the *cys3-Bg* marker is significantly diminished (18% instead of 27%; $P = 0.034$). Both modifications in NMS abolish the gradient of NMS observed in the wild-type strain. We don't know if a modification of the ratio of conversion-type to restoration-type repair, as observed for the *HIS4* locus, contributes to the observed polarity gradient in the wild-type strain at *CYS3*. If this is the case, a steep gradient may reflect an excess of restoration-type over conversion-type repair at the 3′ end of *CYS3*. Another interpretation of this effect, as proposed by Alani *et al.* (1994), is that MMR regulates both the length of heteroduplex DNA and the formation of symmetric heteroduplex DNA. In our *msh2 pms1* strains, the frequency of aberrant 4:4 tetrads at *CYS3* is similar (<1%) to that at *ARG4* and much lower than that at *HIS4* (Alani *et al.* 1994). This result indicates that aberrant 4:4 more likely results from multiple independent events rather than from the processing of DNA intermediates with regions of symmetric heteroduplex.

Our physical analysis of meiotic DSB formation in MMR mutants allowed us to test whether MMR proteins are directly or indirectly involved in the formation of DSBs or in the processing of gene conversion intermediates, apart from their function in the recognition and correction of heteroduplexes containing mispaired bases. Our results indicate that the frequency and the positioning of DSBs in a *msh2 pms1 rad50S* mutant strain is similar (7 ± 1.5%) to that found in the *rad50S* strain. We conclude that MMR proteins are not involved in DSB formation. *MSH2* and *PMS1* could also be implicated indirectly in the resection of DSBs, which would affect both recombination and DSB repair. Using neutral agarose gels, we find that both the intensity of the transient signal and the kinetics are similar in wild-type and *msh2 pms1* strains. We have also analyzed the processing of the 5′ and 3′ strands on alkaline agarose gels with strand-specific riboprobes. In six strains differing with respect to their allelic composition at *CYS3* (*CYS3*/*CYS3*, *cys3-Bg*/*CYS3*, and *cys3-RI*/*CYS3*), and either wild-type or *msh2 pms1*, the 3′ strand exhibits the same length as in the *rad50S* strains (data not shown). We have also examined the 5′ strand. Under our experimental conditions, we did not detect convincing differences in the length of the resected strand among these strains.

The Msh2 protein has been recently shown to bind to synthetic Holliday junctions (Alani *et al.* 1997), which suggests that another stage at which the MMR system could influence recombination is in the formation and resolution of Holliday junctions (for a review see Stahl 1996).

We thank Y. Surdin-Kerjean and L. Grivell or providing pStr1.1 and PM5239 plasmids, respectively, all members of our laboratory for helpful discussion, F. Fabre and G. Simchen for comments about the manuscript, and K. Smith for English grammar corrections. We also thank S. Le Bilcot for her technical assistance. This work was successively performed in the Centre National de la Recherche Scientifique URA1354, URA1292, and UMR144 and has been supported by grants from the Groupement de Recherches et d'Etudes sur les Génomes, the Association de Recherche Contre le Cancer, the Ligue Nationale contre le Cancer, the A.C.C. SV8 program from the Ministère de l'Education Nationale, de l'Enseignement Supérieur, et de la Recherche, the Human Frontier Science Programs (RG493/95), and the European Community (Human Capital Mobility Meiosis Network and Biotech program).

LITERATURE CITED

Alani, A., 1996 The *Saccharomyces cerevisiae* Msh2 and Msh6 proteins form a complex that binds specifically to duplex oligonucleotides containing mismatched DNA base pairs. Mol. Cell. Biol. **16:** 5604–5615.

Alani, E., R. Padmore and N. Kleckner, 1990 Analysis of wild type and *rad50* mutants of yeast suggests an intimate relationship between meiotic chromosome synapsis and recombination. Cell **61:** 419–436.

Alani, E., R. A. G. Reenan and R. D. Kolodner, 1994 Interaction between mismatch repair and genetic recombination in *Saccharomyces cerevisiae*. Genetics **137:** 19–39.

Alani, E., S. Lee, M. F. Kane, J. Griffith and R. D. Kolodner, 1997 *Saccharomyces cerevisiae* MSH2, a mispaired base recognition protein, also recognizes Holliday junctions in DNA. J. Mol. Biol. **265:** 289–301.

Barton, A. B., D. B. Kaback, M. W. Clark, T. Keng, B. F. F. Ouellette *et al.*, 1993 Physical localization of yeast *CYS3*, a gene whose product resembles the rat γ-cystathionase and *Escherichia coli* cystathionine γ-synthase enzymes. Yeast **9:** 363–369.

Baudat, F., and A. Nicolas, 1997 Clustering of meiotic double-strand breaks on yeast chromosome III. Proc. Natl. Acad. Sci. USA **94:** 5213–5218.

Bergerat, A., B. de Massy, D. Gadelle, P.-C. Varoutas, A. Nicolas *et al.*, 1997 An atypical topoisomerase II from archaea with implications for meiotic recombination. Nature **386:** 414–417.

Bishop, D. K., D. Park, L. Xu and N. Kleckner, 1992 *DMC1*: a meiosis-specific yeast homolog of *E. coli recA* required for recombination, synaptonemal complex formation, and cell cycle progression. Cell **69:** 439–456.

Boeke, J. D., F. Lacroute and G. R. Fink, 1984 A positive selection for mutants lacking orotidine-5′-phosphate decarboxylase activity in yeast: 5-fluoroacetic acid resistance. Mol. Gen. Genet. **197:** 345–346.

Borts, R. H., and J. E. Haber, 1987 Meiotic recombination in yeast: alteration by multiple heterozygosities. Science **237:** 1459–1465.

Bullard, S. A., S. Kim, A. M. Galbraith and R. E. Malone, 1996 Double strand breaks at the *HIS2* recombination hotspot in *Saccharomyces cerevisiae*. Proc. Natl. Acad. Sci. USA **93:** 13054–13059.

Cao, L., E. Alani and N. Kleckner, 1990 A pathway for generation and processing of double-strand breaks during meiotic recombination in *S. cerevisiae*. Cell **61:** 1089–1101.

Cherest, H., and Y. Surdin-Kerjan, 1992 Genetic analysis of a new mutation conferring cysteine auxotrophy in *Saccharomyces cerevisiae*: updating of the sulfur metabolism pathway. Genetics **130:** 51–58.

Church, G. M., and W. Gilbert, 1984 Genomic sequencing. Proc. Natl. Acad. Sci. USA **81:** 1991–1995.

Datta, A., M. Hendrix, M. Lipsitch and S. Jinks-Robertson, 1997 Dual roles for DNA sequence identity and the mismatch repair system in the regulation of mitotic crossing-over in yeast. Proc. Natl. Acad. Sci. USA **94:** 9757–9762.

de Massy, B., and A. Nicolas, 1993 The control *in cis* of the position and the amount of the *ARG4* meiotic double-strand break of *Saccharomyces cerevisiae*. EMBO J. **12:** 1459–1466.

de Massy, B., V. Rocco and A. Nicolas, 1995 The nucleotide mapping of DNA double-strand breaks at the *CYS3* initiation site of meiotic recombination in *Saccharomyces cerevisiae*. EMBO J. **14:** 4589–4598.

Detloff, P., and T. D. Petes, 1992 Measurements of excision repair

tracts formed during meiotic recombination in *Saccharomyces cerevisiae*. Mol. Cell. Biol. **12:** 1805–1814.

Detloff, P., M. A. White and T. D. Petes, 1992 Analysis of a gene conversion gradient at the *HIS4* locus in *Saccharomyces cerevisiae*. Genetics **132:** 113–123.

Fan, Q.-Q., and T. D. Petes, 1996 Relationship between nuclease-hypersensitive sites and meiotic recombination hotspot activity at the *HIS4* locus of *Saccharomyces cerevisiae*. Mol. Cell. Biol. **16:** 2037–2043.

Fan, Q.-Q., F. Xu and T. D. Petes, 1995 Meiosis-specific double-strand DNA breaks at the *HIS4* recombination hotspot in the yeast *Saccharomyces cerevisiae*: control in *cis* and *trans*. Mol. Cell. Biol. **15:** 1679–1688.

Fogel, S., D. D. Hurst and R. K. Mortimer, 1971 Gene conversion in unselected tetrads from multipoint crosses. The Second Stadler Symposia pp. 89–110.

Fogel, S., R. K. Mortimer and K. Lusnak, 1981 Mechanism of meiotic gene conversion or "wandering on a foreign strand," pp. 289–339 in *The Molecular Biology of Yeast Saccharomyces*, edited by J. N. Strathern, J. E. Jones and J. Broach. Cold Spring Harbor Laboratory Press, Cold Spring Harbor, NY.

Goldway, M., A. Sherman, D. Zenvirth, T. Arbel and G. Simchen, 1993 A short chromosomal region with major roles in yeast chromosome III meiotic disjunction, recombination and double strand breaks. Genetics **133:** 159–169.

Hastings, P. J., 1984 Measurement of restoration and conversion: its meaning for the mismatch repair hypothesis of conversion. Cold Spring Harbor Symp. Quant. Biol. **49:** 49–53.

Keeney, S., and N. Kleckner, 1996 Communication between homologous chromosomes: genetic alterations at a nuclease-hypersensitive site can alter mitotic chromatin structure at that site both in *cis* and in *trans*. Genes Cells **1:** 475–489.

Keeney, S., C. Giroux and N. Kleckner, 1997 Meiosis-specific DNA double-strand breaks are catalyzed by Spo11, a member of a widely conserved protein family. Cell **88:** 375–384.

Kirkpatrick, D. T., M. Dominska and T. D. Petes, 1998 Conversion-type and restoration-type repair of DNA mismatches formed during meiotic recombination in *Saccharomyces cerevisiae*. Genetics **149:** 1693–1705.

Klein, S., D. Zenwirth, V. Dror, A. B. Barton, D. B. Kaback *et al.*, 1996 Patterns of meiotic double-strand breakage on native and artificial yeast chromosomes. Chromosoma **105:** 205–284.

Kramer, W., B. Kramer, M. Williamson and S. Fogel, 1989 Cloning and nucleotide sequence of DNA mismatch repair gene *PMS1* from *Saccharomyces cerevisiae*: homology of PMS1 to procaryotic MutL and HexB. J. Bacteriol. **171:** 5339–5346.

Lichten, M., and A. S. H. Goldman, 1995 Meiotic recombination hotspots. Annu. Rev. Genet. **29:** 423–444.

Lichten, M., C. Goyon, N. P. Schultes, D. Treco, J. W. Szostak *et al.*, 1990 Detection of heteroduplex DNA molecules among the products of *Saccharomyces cerevisiae* meiosis. Proc. Natl. Acad. Sci. USA **87:** 7653–7657.

Malone, R. E., S. Bullard, S. Lundquist, S. Kim and T. Tarkowski, 1992 A meiotic gene conversion gradient opposite to the direction of transcription. Nature **359:** 154–155.

Malone, R. E., S. Kim, S. A. Bullard, S. Lundsquist, L. Hutchings-Crow *et al.*, 1994 Analysis of a recombination hotspot for gene conversion occurring at the *HIS2* gene of *Saccharomyces cerevisiae*. Genetics **137:** 5–18.

Mao-Draayer, Y., A. M. Galbraith, D. L. Pittman, M. Cool and R. E. Malone, 1996 Analysis of meiotic recombination pathways in *Saccharomyces cerevisiae*. Genetics **144:** 71–86.

Marsischky, G. T., N. Filosi, M. F. Kane and R. Kolodner, 1996 Redundancy of *Saccharomyces cerevisiae MSH3* and *MSH6* in *MSH2*-dependent mismatch repair. Genes Dev. **10:** 407–420.

Nag, D. K., and T. D. Petes, 1993 Physical detection of heteroduplexes during meiotic recombination in the yeast *Saccharomyces cerevisiae*. Mol. Cell. Biol. **13:** 2324–2331.

Nicolas, A., and T. D. Petes, 1994 Polarity of meiotic gene conversion in fungi: contrasting views. Experientia **50:** 242–252.

Nicolas, A., and J. L. Rossignol, 1989 Intermediates in homologous recombination revealed by marker effects in *Ascobolus*. Genome **31:** 528–535.

Nicolas, A., D. Treco, N. P. Schultes and J. W. Szostak, 1989 An initiation site for meiotic gene conversion in the yeast *Saccharomyces cerevisiae*. Nature **338:** 35–39.

Ohta, K., T. Shibata and A. Nicolas, 1994 Changes in chromatin structure at recombination initiation sites during yeast meiosis. EMBO J. **13:** 5754–5763.

Ono, B. I., K. Tanaka, K. Naito, C. Heike, S. Shinoda *et al.*, 1992 Cloning and characterization of the *CYS3* (*CYI1*) gene of *Saccharomyces cerevisiae*. J. Bacteriol. **174:** 3339–3347.

Ouellette, B. F., M. W. Clark, T. Keng, R. G. Storms, W. Zhong *et al.*, 1993 Sequencing of chromosome I from *Saccharomyces cerevisiae*: analysis of a 32 kb region between the *LTE1* and *SPO7* genes. Genome **36:** 32–42.

Petes, T. D., R. E. Malone and L. S. Symington, 1991 Recombination in yeast, pp. 407–521 in *The Molecular and Cellular Biology of the Yeast Saccharomyces*, edited by R. Broach, E. W. Jones and J. R. Pringle. Cold Spring Harbor Laboratory Press, Cold Spring Harbor, NY.

Prolla, T. A., Q. Pang, E. Alani, R. D. Kolodner and R. M. Liskay, 1994 MLH1, PMS1, and MSH2 interactions during the initiation of DNA mismatch repair in yeast. Science **265:** 1091–1093.

Reenan, R., and R. Kolodner, 1992a Isolation and characterization of two *Saccharomyces cerevisiae* genes encoding homologs of the bacterial HexA and MutS mismatch repair proteins. Genetics **132:** 963–973.

Reenan, R., and R. Kolodner, 1992b Characterization of insertion mutation in the *Saccharomyces cerevisiae MSH1* and *MSH2* genes: evidence for separate mitochondrial and nuclear functions. Genetics **132:** 975–985.

Rocco, V., and A. Nicolas, 1996 Sensing of nonhomology lowers the initiation of meiotic recombination in yeast. Genes Cells **1:** 645–661.

Scherer, S., and R. W. Davis, 1979 Replacement of chromosome segments with altered DNA sequences constructed *in vitro*. Proc. Natl. Acad. Sci. USA **76:** 4951–4955.

Schultes, N. P., and J. W. Szostak, 1990 Decreasing gradients of gene conversion on both sides of the initiation site for meiotic recombination at the *ARG4* locus in yeast. Genetics **126:** 813–822.

Schwacha, A., and N. Kleckner, 1995 Identification of double Holliday junctions as intermediates in meiotic recombination. Cell **83:** 783–791.

Stahl, F., 1996 Meiotic recombination in yeast: coronation of the double-strand break repair model. Cell **87:** 965–968.

Sun, H., D. Treco, N. P. Schultes and J. W. Szostak, 1989 Double-strand breaks at an initiation site for meiotic gene conversion. Nature **338:** 87–90.

Sun, H., D. Treco and J. W. Szostak, 1991 Extensive 3′-overhanging, single-stranded DNA associated with the meiosis-specific double-strand breaks at the *ARG4* recombination initiation site. Cell **64:** 1155–1161.

Szostak J. W., T. L. Orr-Weaver, R. J. Rothstein and F. W. Stahl, 1983 The double-strand break repair model for conversion and crossing-over. Cell **33:** 25–35.

Whitehouse, H. L. K., 1982 *Genetic Recombination, Understanding the Mechanisms*. John Wiley & Sons, Chichester.

Wilson, C., J. D. M. Chao, A. N. Imbalzano, G. R. Schnitzler, R. E. Kingston *et al.*, 1996 RNA polymerase II holoenzyme contains SWI/SNF regulators involved in chromatin remodeling. Cell **88:** 235–244.

Wu, T.-C., and M. Lichten, 1994 Meiosis-induced double-strand break sites determined by yeast chromatin structure. Science **263:** 515–518.

Xu, F., and T. D. Petes, 1996 Fine-structure mapping of meiosis-specific double-strand DNA breaks at a recombination hotspot associated with an insertion of telomeric sequence upstream of the *HIS4* locus in yeast. Genetics **143:** 1115–1125.

Zahn-Zabal, M., and J. Kohli, 1996 The distance dependence of the fission yeast *ade6-M26* marker effect in two-factor crosses. Curr. Genet. **29:** 530–536.

Zenvirth, D., T. Arbel, A. Sherman, M. Golway, S. Klein *et al.*, 1992 Multiple sites for double-strand breaks in whole meiotic chromosomes of *Saccharomyces cerevisiae*. EMBO J. **11:** 3441–3447.

Communicating editor: S. Jinks-Robertson